Derivation of Log-Likelihood Ratio for M-ary Non-Orthogonal FSK Wireless System

Daisuke Nojima, Yuhei Nagao, Masayuki Kurosaki and Hiroshi Ochi

Faculty of Computer Science and Systems Engineering, Kyushu Institute of Technology
Kawazu 680-4 Iizuka, Fukuoka, 820-8502, JAPAN
Email: {nojima, nagao, kurosaki, ochi}@dsp.cse.kyutech.ac.jp

***Abstract*—In a soft decision Viterbi decoder, the log-likelihood ratio (LLR) metric is used to improve the performance of the error correction. On linear systems under additive white gaussian noise channel, this is straightforward as the error distribution at the input of the Viterbi decoder is also gaussian. In non-linear systems such as the M-ary non-coherent non-orthogonal frequency shift keying (FSK), this is generally not true. However, non-orthogonal non-coherent FSK LLR has not yet been proposed in literature. In this paper we derived the LLR for the M-ary non-orthogonal FSK mathematically and verified it using simulations.**

***Index Terms*—Soft Decision Viterbi Decoder, Log-Likelihood Ratio, M-ary Non-Orthogonal FSK Wireless System**

I. Introduction

Recently, in order to further improve the quality of communication and reduce manufacturing cost, wireless communication has adopted digital modulation to replace analog modulation. For instance, frequency modulation (FM) which is an analog modulation scheme used in the wireless communication system can be modified into a digital modulation scheme called frequency shift keying (FSK). Previous FM systems can be converted to an FSK wireless communication system simply by replacing the analog baseband portion to digital FSK. The voltage-controlled oscillator (VCO) circuit and the remaining radio frequency (RF) analog components can still be used in the new system. FSK wireless communication system is widely used in radio transceiver systems. For instance, it has been used in taxi, police, and firefighter radio communication system in Japan, America, and Europe [1]–[4].

Based on the frequency shifts, there are two types of FSK methods, M-ary orthogonal FSK and non-orthogonal FSK [5]. The main advantage of non-orthogonal FSK system is that it has better spectral efficiency than M-ary orthogonal FSK. This is because the minimum frequency interval can be less than the symbol rate. In this paper, we pay attention to M-ary non-orthogonal FSK system.

The algorithms presented in this paper will be applied to the forward error correction (FEC) mechanism found in digital FSK systems. Specifically we are concerned with, the convolutional encoder found in the transmitter and the Viterbi decoder in the receiver for error correction. In the method of Viterbi decoder, there are hard decision Viterbi decoder and soft decision Viterbi decoder [6]. Soft decision Viterbi decoders generally perform better than hard decision Viterbi decoders due to the lesser quantization errors. Furthermore, soft decision Viterbi decoders may use a much better metric known as the log-likelihood ratio (LLR) compared to the hamming distance metric of the hard decision Viterbi or the Euclidian distance metric of conventional soft decision Viterbi decoders [7].

Unfortunately, unlike linear receivers such as amplitude shift keying (ASK) or phase shift keying (PSK) based systems, FSK is a non-linear receiver. The conventional LLR, that is LLR of linear receivers are derived from Gaussian distribution. However, error distribution before entering the Viterbi decoder of FSK wireless communication system is a non-Gaussian distribution, because FSK is a non-linear receiver. Based on the distribution of the noise, the corresponding LLR equation for the Viterbi decoder also changes. In [8], the LLR of M-ary orthogonal FSK system was presented using a non-Gaussian error assumption. This results in significant increase in performance compared to conventional LLR systems which assumes that the noise has Gaussian distribution.

The purpose of this paper is to derive LLR for the M-ary non-orthogonal FSK wireless communication system. Because orthogonal FSK and non-orthogonal FSK, uses a different receiver architecture, the error distribution before entering the Viterbi decoder in [8] cannot be used for non-orthogonal FSK.

The rest of the paper is organized as follows. Section II shows the non orthogonal FSK wireless system in detail. In Section III, we derive the probability density function (pdf) which considers the non-linear characteristic of the frequency discriminator which is non-coherent demodulator. In section IV and V, we apply the modified LLR for FSK wireless system and shows simulation results in Rayleigh fading environment. Finally, section VI presents the conclusions of this research.

II. System Outline

In this paper, we use the frequency discriminator of non-coherent detection for the M-ary non-orthogonal FSK system [9].

The FSK transmitted signal $x(t)$ is shown in eq. (1). $s(t)$ is the transmitted symbol and Δf is the frequency interval parameter.

$$x(t) = \exp(j2\pi s(t)\Delta f t) \tag{1}$$

978-1-4673-1881-5/12/$31.00 ©2012 IEEE

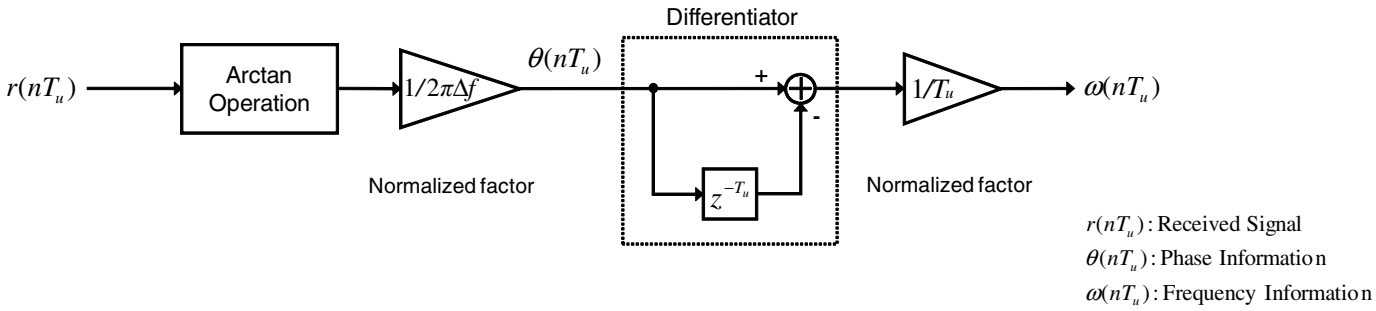

Fig. 1. Frequency Discriminator Architecture

We assumed that the transmission frequency bandwidth is narrow such that the channel is a Rayleigh flat fading channel. The received signal $r(t)$ is shown in eq. (2). The additive white Gaussian noise $w(t)$ in-phase component and quadrature-phase component are Gaussian distributed with zero mean and variance $\sigma^2/2$. The Rayleigh flat fading coefficient $h(t)$ is composed of the amplitude component $A(t)$ phase component $\psi(t)$.

$$r(t) = A(t)\exp(j2\pi s(t)\Delta f t + \psi(t)) + w(t) \tag{2}$$

$$h(t) = A(t)\exp(j\psi(t)) \tag{3}$$

In eq. (4), the received signal $r(t)$ from eq. (2) is sampled every T_u seconds. Note that the sampling time T_u is small compared with the symbol time T_s. R is the upsampling rate.

$$r(nT_u) = A(nT_u)\exp\{j2\pi s(nT_u)\Delta f n T_u + \psi(nT_u)\} + w(nT_u)$$

where

$$T_s = R \cdot T_u \tag{4}$$

Fig. 1 shows the frequency discriminator architecture. In the frequency discriminator, the input signal is converted from rectangular coordinate to polar coordinate using the arctan operation in order to extract the phase information from the received signal $r(nT_u)$. The output of arctan operation $\theta(nT_u)$ is shown in eq. (5). $\theta(nT_u)$ is phase information. Here, the Gaussian noise $w(nT_u)$ is converted to phase error $\phi(nT_u)$ due to the arctan operation.

$$\theta(nT_u) = s(nT_u)nT_u + \psi(nT_u) + \phi(nT_u) \tag{5}$$

This phase error $\phi(nT_u)$ goes to the differentiator which transforms $\phi(nT_u)$ to the frequency error $e(nT_u)$. Using the approximations in eq. (7), the output of differentiator $\omega(nT_u)$ is shown in eq. (6). Note that $\omega(nT_u)$ is the frequency information. The error information is converted from phase error $\phi(nT_u)$ to frequency error $e(nT_u)$ using the differentiator.

$$\begin{aligned}\omega(nT_u) &= \theta(nT_u) - \theta\{(n-1)T_u\} \\ &= s(nT_u) + e(nT_u),\end{aligned} \tag{6}$$

where

$$\begin{aligned}\psi(nT_u) &\approx \psi\{(n-1)T_u\}, \\ s(nT_u) &\approx s\{(n-1)T_u\}.\end{aligned} \tag{7}$$

Because the distribution of the additive noise $w(nT_u)$ changes due to the nonlinearity of frequency discriminator, we need to derive the pdf of phase error $\phi(nT_u)$ and frequency error $e(nT_u)$.

III. LLR of Non-coherent Detection for M-ary Non-orthogonal FSK Signal

A. Log-likelihood Ratio

The LLR of the bit information s_j of the j^{th} transmission symbol s is given by eq. (8).

$$\mathrm{LLR}(s_j) = \log\left(\frac{p(s_j = 1|r)}{p(s_j = 0|r)}\right) \tag{8}$$

From eq. (8), we apply Bayes' theorem to obtain eq. (9) [10]. Note that A_j is the set of all transmit symbols in which the j^{th} bit information is one while B_j is the set in which the j^{th} bit information is zero.

$$\mathrm{LLR}(s_j) = \log\left(\frac{\sum_{A_j \in \{Z|s_j=1\}} p(r|s_j = 1)}{\sum_{B_j \in \{Z|s_j=0\}} p(r|s_j = 0)}\right) \tag{9}$$

B. Probability Density Function of Phase Error

In this part, the pdf of the phase error $\phi(nT_u)$ from the output of the arctan operation in the frequency discriminator is explained.

$A(t)$ of received signal is replaced by A for simplicity. Assuming that the received signal amplitude is unity as shown in Fig. 2. In Fig. 2, we can see how the phase of the receive signal are related with the amplitude of the received signal and noise power. Here we assume that the amplitude of the received signal is $r_0 = A$ while the noise $w(nT_u)$ is complex Gaussian distributed with zero mean and variance of $\sigma^2/2$.

This model is clearly similar to a Nakagami Rice fading model with $r(nT_u)$ as the dominant line-of-sight (LOS) component while the noise is analogous to the weaker various reflected components that follow rayleigh distribution. Using this analogy, we infer that the phase error distribution at the

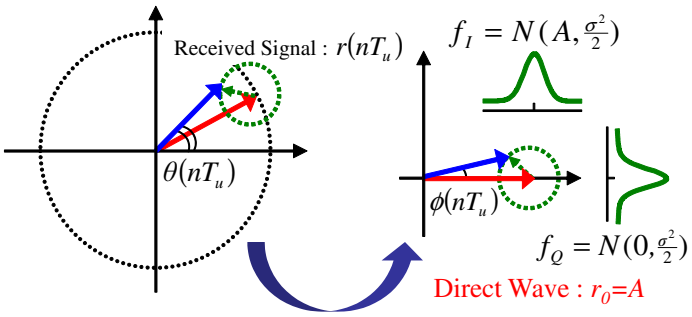

Fig. 2. Received Signal Model

output of the arctan operation follows the phase distribution of the Nakagami Rice fading.

The random variable of phase error is assumed to be ϕ. The pdf of the phase of Nakagami-Rice fading $f_\phi(\phi)$ is shown in eq. (10) [11]–[13].

$$f_\phi(\phi) = \frac{1}{2\pi}\exp\left(-\frac{A^2}{2\sigma^2}\right)\left[1+\sqrt{\frac{\pi}{2}}\frac{A\cos\phi}{\sigma}\cdot \exp\left(\frac{A^2\cos^2\phi}{2\sigma^2}\right)\left\{1+\mathrm{erf}\left(\frac{A\cos\phi}{\sqrt{2}\sigma}\right)\right\}\right] \quad (10)$$

C. Probability Density Function of Frequency Error

In this part, we examine the pdf of the frequency error $e(nT_u)$ from the output of the differentiator operation. In Fig. 1, we see that the frequency error $e(nT_u)$ depends on the difference between the adjacent samples of the phase error $\phi(nT_u)$ and $\phi\{(n-1)T_u\}$. In order to derive the distribution of the frequency error, we consider the correlation of $\phi(nT_u)$ and $\phi\{(n-1)T_u\}$.

First, the phase error is assumed to have a flat frequency spectrum. Then, bandwidth limitation is performed by the band-limited filter in the receiver's first stage. Band-limited auto-correlation characteristic $\alpha(\tau)$ of the white noise is shown in eq. (11). Here τ is the discrete-time index, B is the filter bandwidth, and σ^2 is the energy of noise, respectively.

$$\alpha(\tau) = E[\phi(nT_u)\phi\{(n-\tau)T_u\}] = B\sigma^2\frac{\sin(\pi B\tau)}{\pi B\tau} \quad (11)$$

Here, we define the random variable of the phase error $\phi(nT_u)$ as ϕ_0 and $\phi\{(n-1)T_u\}$ as ϕ_{T_u}. The random variable ϕ_0 and ϕ_{T_u} has high correlation. This high correlation is a necessary consideration when deriving the pdf of the frequency error because of oversampling and band-limited filtering. Note that the value of the coefficient of correlation does not depend on signal-noise ratio (SNR). But, it depends on frequency bandwidth B and sampling time T_u.

The random variable ϕ_{T_u} can be represented as two random variables as shown in eq. (12) [14].

$$\phi_{T_u} = \alpha(T_u)\phi_0 + \sqrt{\alpha(0)-\alpha(T_u)^2}\delta \quad (12)$$

Where $\alpha(T_u)$ is the correlation of the random variables ϕ_0 and ϕ_{T_u}. Note that ϕ_0 and δ are independent. The new random variable δ also has the phase distribution of Nakagami-Rice fading. When the sampling time T_u between the signals is increased, the correlation between the signals disappears and $\alpha(T_u)$ decreases. When $\alpha(T_u)$ is small, the influence of the random variable ϕ_0 also decreases and the random variable ϕ_{T_u} is now mostly dictated by δ.

The random variable of the frequency error represented as e is calculated from the finite difference of $\phi(nT_u)$ and $\phi(n-1)T_u$. This is shown in eq.(13).

$$e = \phi_0 - \phi_{T_u} = \{1-\alpha(T_u)\}\phi_0 - \sqrt{\alpha(0)-\alpha(T_u)^2}\delta \quad (13)$$

We then derive the pdf of random variable e. Again, we apply a change of variables in eq. (14).

$$\begin{aligned} e &= e(\phi_0,\delta) = \{1-\alpha(T_u)\}\phi_0 - \sqrt{\alpha(0)-\alpha(T_u)^2}\delta \\ u &= u(\phi_0,\delta) = \phi_0 \end{aligned} \quad (14)$$

Now, let the joint pdf [15] of the random variable e and u be $\psi(e,u)$. Correspondingly, the marginal distribution of e is represented as $g(e)$. Finally, the pdf of frequency error $g(e)$ is shown in eq. (15).

$$g(e) = \int_{-\infty}^{\infty}\psi(e(\phi_0,\delta),u(\phi_0,\delta))du \quad (15)$$

From eq. (14), we define the following functions.

$$\begin{aligned} \delta &= \frac{1-\alpha(T_u)}{\sqrt{\alpha(0)-\alpha(T_u)^2}}u - \frac{1}{\sqrt{\alpha(0)-\alpha(T_u)^2}}e \\ \phi_0 &= u \end{aligned} \quad (16)$$

In order to solve eq. (15), we will use the Jacobian matrix identify shown in eq. (17) [16].

$$J = \begin{vmatrix} \frac{\partial\delta}{\partial e} & \frac{\partial\delta}{\partial u} \\ \frac{\partial\phi_0}{\partial e} & \frac{\partial\phi_0}{\partial u} \end{vmatrix} = -\frac{1}{\sqrt{\alpha(0)-\alpha(T_u)^2}} \quad (17)$$

Since the random variable ϕ and δ are independent, the pdf can be separated. The pdf of ϕ is designated as $f_\phi(\phi)$ while the pdf of δ is designated as $f_\delta(\delta)$. The result of marginal pdf of ϕ and δ are then shown in eq. (18). The pdf of the frequency error $g(e)$ is shown in eq. (19) from eq. (18).

Using eq. (9) and (19), the LLR of non-coherent detection for M-ary non-orthogonal FSK signal is shown eq. (20).

$$\mathrm{LLR}(s_j) = \log\left(\frac{\sum_{A_j\in\{Z|s_j=1\}}g(\omega|s_j=1)}{\sum_{B_j\in\{Z|s_j=0\}}g(\omega|s_j=0)}\right) \quad (20)$$

$$g(e) = \int_{-\infty}^{\infty} f\left(\frac{1-\alpha(T_u)}{\sqrt{\alpha(0)-\alpha(T_u)^2}}\phi_0 - \frac{e}{\sqrt{\alpha(0)-\alpha(T_u)^2}}, \phi_0\right)|J|\, d\phi$$
$$= \int_{-\infty}^{\infty} f_\delta\left(\frac{1-\alpha(T_u)}{\sqrt{\alpha(0)-\alpha(T_u)^2}}\phi_0 - \frac{e}{\sqrt{\alpha(0)-\alpha(T_u)^2}}\right) f_\phi(\phi_0)\frac{1}{\sqrt{\alpha(0)-\alpha(T_u)^2}} d\phi \quad (18)$$

$$g(e) = \int_{\phi_{min}}^{\phi_{max}} \frac{1}{2\pi}\exp\left(-\frac{A^2}{2\sigma^2}\right)\left[1+\sqrt{\frac{\pi}{2}}\frac{A\cos(\phi_0'-e')}{\sigma}\exp\left(\frac{A^2\cos^2(\phi_0'-e')}{2\sigma^2}\right)\left\{1+\mathrm{erf}\left(\frac{A\cos(\phi_0'-e')}{\sqrt{2}\sigma}\right)\right\}\right]\cdot$$
$$\frac{1}{2\pi}\exp\left(-\frac{A^2}{2\sigma^2}\right)\left[1+\sqrt{\frac{\pi}{2}}\frac{A\cos\phi_0}{\sigma}\exp\left(\frac{A^2\cos^2\phi_0}{2\sigma^2}\right)\left\{1+\mathrm{erf}\left(\frac{A\cos\phi_0}{\sqrt{2}\sigma}\right)\right\}\right]\frac{1}{\sqrt{\alpha(0)-\alpha(T_u)^2}}d\phi$$

where

$$\phi_0' = \frac{1-\alpha(T_u)}{\sqrt{\alpha(0)-\alpha(T_u)^2}}\phi_0, \quad e' = \frac{e}{\sqrt{\alpha(0)-\alpha(T_u)^2}}. \quad (19)$$

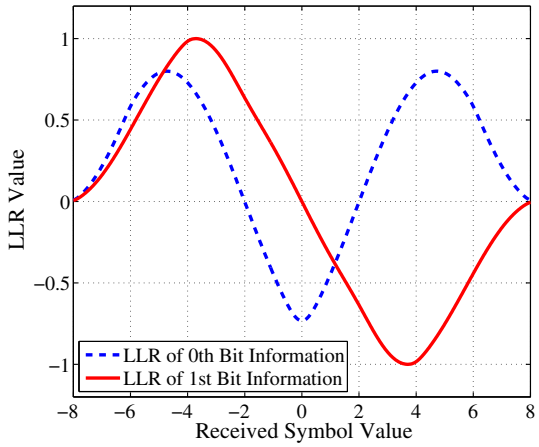

Fig. 3. LLR for FSK System Based on ARIB STD T-98 (SNR = 10 [dB]).

TABLE I
SYSTEM PARAMETERS BASED ON ARIB STD T-98

Parameters	Value
Modulation	4-ary FSK Modulation
Symbol Time T_s	416.7 [μs]
Sampling Time T_u	52.1 [μs]
Frequency BandWidth B	4800 [Hz]
Carrier Frequency	467 [MHz]

TABLE II
SYMBOL MAPPING FOR ARIB STD T-98

Symbol s	1^{st} bit Information	0^{th} bit Information
+3	0	1
+1	0	0
-1	1	0
-3	1	1

TABLE III
SIMULATION PARAMETERS

Parameters	Value
Number of DATA bit	400 [bit] (1 [Packet])
Number of Packet	5000 [Packet]
Simulation Environment	Rayleigh fading channel
Frame Synchronization	Perfect
Coding Rate	2/3
Doppler Frequency	12.9, 25.8, 43.2 [Hz] (30, 60, 100 [km/h])

IV. VERIFICATION FOR 4-ARY FSK WIRELESS SYSTEM

In this section, we applied the pdf of frequency error and modified LLR for 4-ary FSK wireless system based on ARIB STD T-98 [1]. Table I lists the system parameters based on ARIB STD T-98.

We apply the modified LLR for 4-ary FSK wireless system from eq. (20). Table II lists the symbol mapping for this system. The 0^{th} bit information s_0 and 1^{st} bit information s_1 of transmitted signals s is given by eq. (21).

$$\mathrm{LLR}(s_0) = \log\left(\frac{g_3(e)+g_{-3}(e)}{g_1(e)+g_{-1}(e)}\right)$$
$$\mathrm{LLR}(s_1) = \log\left(\frac{g_{-3}(e)+g_{-1}(e)}{g_3(e)+g_1(e)}\right) \quad (21)$$

Here, "$g_3(e)$", "$g_1(e)$", "$g_{-1}(e)$", "$g_{-3}(e)$" represents the probability density function of transmission symbols $+3(01_2)$, $+1(00_2)$, $-1(10_2)$, and $-3(11_2)$, respectively [1]. Fig. 3 shows the LLR curve according to eq. (21). If the LLR value of the received signal is positive, there is a high probability that the bit value is "1". On the other hand, if the LLR value of the received signal is negative, there is a high probability that the transmitted bit is "0". The LLR values computed are then passed into the soft decision Viterbi decoder.

V. SIMULATION RESULT

In this part, we performed simulations with Rayleigh fading channel environment. Table III lists the rest of simulation parameters of all environment. Firstly, we investigate the appropriate number of soft decision bits by simulations. Fig. 4 shows PER characteristic at the number of soft decision bits of 20, 25 and 30 dB. In Fig. 4, we see the saturated PER characteristic of 12bit quantized soft decision Viterbi decoder

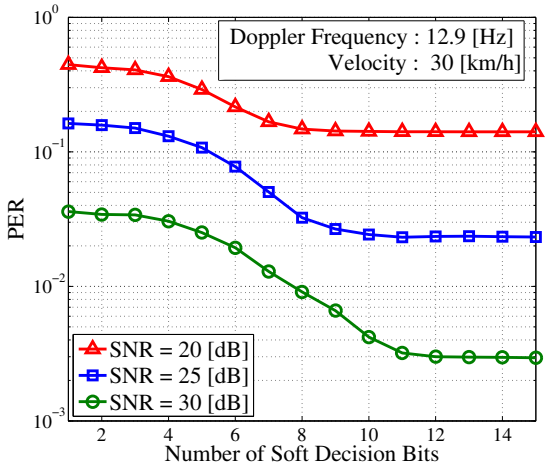

Fig. 4. PER Characteristic of Change Number of Soft Decision bits (Maximum Doppler frequency : 12.9 [Hz], SNR = 20, 25 and 30 [dB]).

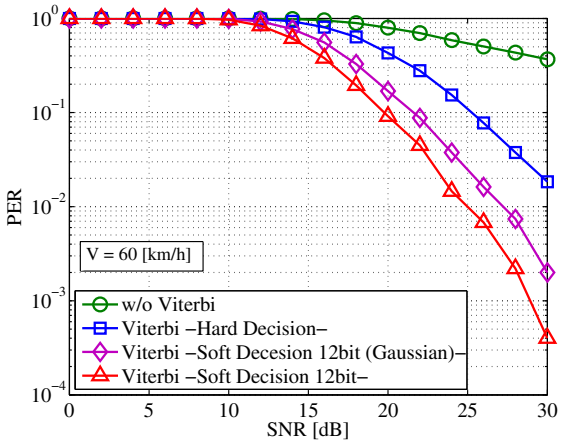

Fig. 5. PER Characteristic (Maximum Doppler Frequency : 25.8 [Hz]).

in 20, 25 and 30 dB cases. Hence, we only considered 12bit quantization for Rayleigh fading channels.

Figs. 5 and 6, shows the PER characteristic in the cases when the velocity is 60 and 100 km/h, respectively.

From Figs. 5 and 6, we see that the case without Viterbi decoder and hard decision Viterbi decoder compared to the case with soft decision Viterbi decoder shows that the latter has improved PER performance. We also see that the PER performance of the uncoded case has a high error floor. On the other hand, we see that the soft decision Viterbi decoder has no visible error floor. We also see that the case of conventional 12bit quantized LLR compared to the case with proposed 12bit quantized LLR has at least 2 dB PER performance improvement.

VI. CONCLUSION

In this paper, we have presented a modified LLR which considers the non-coherent detection like frequency discriminator of M-ary non-orthogonal FSK wireless system. The simulation results in Rayleigh fading environments confirm

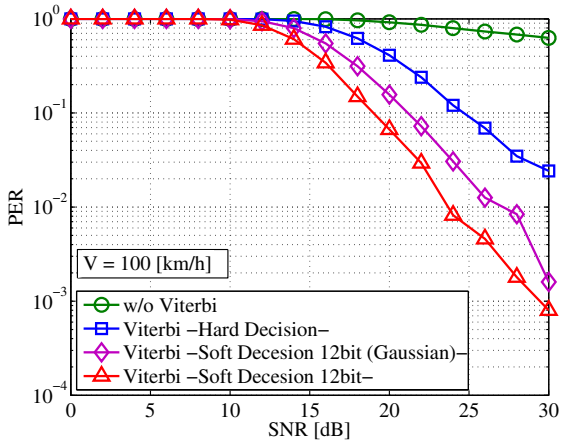

Fig. 6. PER Characteristic (Maximum Doppler Frequency : 43.2 [Hz]).

that performance is improved by using the soft decision Viterbi decoder using modified LLR. For the future work, we will do an RTL design of the proposed modified LLR method.

REFERENCES

[1] ARIB STD-T98, "Digital Convenience Radio Equipment for Simplified Service," Association of Radio Industries and Businesses, 2009.

[2] ETSI TS 102 361-1, "Electromagnetic compatibility and Radio spectrum Matters (ERM); Digital Mobile Radio (DMR) Systems; Part 1: DMR Air Interface (AI) protocol," European Telecommunications Standards Institute, 2006.

[3] ETSI TS 102 490, "Electromagnetic compatibility and Radio spectrum Matters (ERM); Peer-to-Peer Digital Private Mobile Radio using FDMA with a channel spacing of 6,25 kHz with e.r.p. of up to 500 mW," European Telecommunications Standards Institute, 2007.

[4] TIA TIA102, "Project 25 FDMA – Common Air Interface New Technology Standards Project – Digital Radio Technical Standards," Telecommunications Industry Association, 2003.

[5] A. Goldsmith, ed., Wireless Communications, Cambridge University Press, Cambridge, 2005.

[6] A. J. Viterbi, "Convolutional Codes and Their Performance in Communication Systems," *IEEE Trans. Communications*, vol. 19, no. 5, pp. 752–772, Oct. 1971.

[7] T. Kailath, "A general likelihood-ratio formula for signals in Gaussian noise," *IEEE Trans. Information Theory*, vol. 15, no. 3, pp. 350–361, May 1969.

[8] M. K. Simon and R. Annavajjala, "On the optimality of bit detection of certain digital modulations," *IEEE Trans. Communications*, vol. 53, no. 2, pp. 299–307, Feb. 2005.

[9] R. Petrovic and A. F. Molisch, "Reduction of multipath effects for FSK with frequency-discriminator detection," in *Proc. Personal, Indoor, Mobile and Radio Communications '97.*, The 8th IEEE International Symposium on, pp. 943–948, Sept. 1997.

[10] J. G. Proakis, ed., Digital Communications, McGraw-Hill, New York, 1995.

[11] J. D. Parsons, ed., The Mobile Radio Propagation Channel, Wiley, New York,1992.

[12] D. Middleton, ed., An Introduction to Statistical Communication Theory, McGraw-Hill, New York, 1960.

[13] M. Nakagami, "The *m*-Distribution a General Formula of Intensity of Rapid Fading," in W. G. Hoffman, ed., Statistical Methods in Radio Wave Propagation, Permagon Press, Oxford, 1960.

[14] J. Pitman, ed., Probability : Springer Texts in Statistics, Springer, Berlin, 1997.

[15] S. L. Miller and D. G. Childers, ed., Probability and Random Processes : With Applications to Signal Processing and Communications, Academic Press, Waltham, 2004.

[16] M. Spivak, ed., Calculus On Manifolds : A Modern Approach To Classical Theorems Of Advanced Calculus, Westview Press, Boulder, 1971.